

**Contributing Editors**

Emmanuel Fritsch, CNRS, Team 6502, Institut des Matériaux Jean Rouxel (IMN),  
University of Nantes, France (fritsch@cnsr.imn.fr)

Kenneth Scarratt, GIA, Bangkok (ken.scarratt@gia.edu)

**COLORED STONES AND ORGANIC MATERIALS**

**Demantoid from Baluchistan province in Pakistan.** Demantoid garnet can be broadly divided into two petrogenetic groups, namely skarn-hosted and serpentinite-hosted demantoid. Those in the latter group represent the classic localities in the Russian Urals and at Val Malenco, Italy, in addition to sources such as Iran's Kerman province and the Kaghan Valley area in the Hazara district of Pakistan. The serpentinite formations hosting these demantoids are the result of relatively low-grade hydrothermal/metamorphic alteration of ultramafic parent rocks.

Nine demantoids reportedly from a new deposit in the Khuzdar area in Pakistan's Baluchistan province were recently examined in GIA's Carlsbad lab (figure 1). The material was bought by one of these contributors (VP) from a gem merchant based in Peshawar, Pakistan.

*Figure 1. These nine Pakistani demantoids showed dodecahedral form, magnetite inclusions, and asbestiform chrysotile masses on some crystal faces. The smallest stone (bottom left) is 5.2 mm wide, and the largest (top left) is 9.9 mm wide. Photo by Don Mengason.*

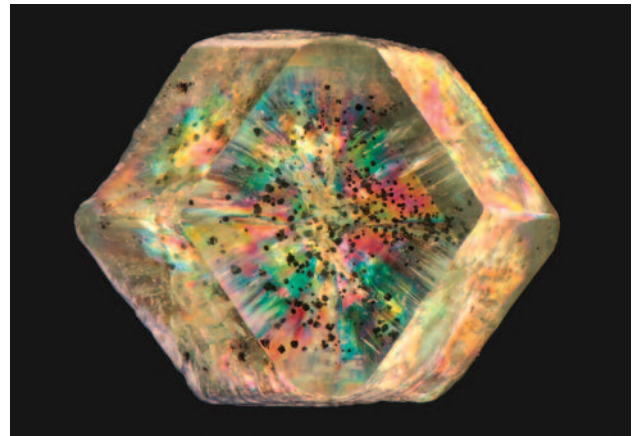


*Figure 2. This demantoid is viewed through a polished window that is roughly parallel to the (110) crystal face. The sample was photographed with cross-polarized lighting and immersed in methylene iodide to highlight the anomalous birefringence. The sample measures 8.8 mm across. Photomicrograph by Aaron Palke.*

The nine rough samples described here (1.74–3.73 ct) all exhibited well-developed crystal faces with typical dodecahedral form. Their color ranged from yellowish green to green, with yellow cores in a few samples. Each showed anomalous birefringence, often with a well-defined “octahedral” pattern (figure 2).

*Editors' note: Interested contributors should send information and illustrations to Justin Hunter at [justin.hunter@gia.edu](mailto:justin.hunter@gia.edu) or GIA, The Robert Mouawad Campus, 5345 Armada Drive, Carlsbad, CA 92008.*

GEMS & GEMOLOGY, VOL. 50, No. 4, pp. 302–315.

© 2014 Gemological Institute of America

Several of the garnets had fibrous (asbestiform) masses of chrysotile adhering to one or more crystal faces, confirming their origin in a serpentinite deposit. Windows were polished into several of these samples for microscopic examination of their internal features. Inclusions of chrysotile fibers (i.e., horsetail inclusions) are concentrated around the rim and radiate out toward the crystal faces (again, see figure 2). The cores of many samples were marked by a field of opaque, equant black inclusions initially presumed to be chromite (figure 3), a commonly observed inclusion in serpentinite-hosted demantoid.

However, laser ablation-inductively coupled plasma-mass spectrometry (LA-ICP-MS) analysis of one of these grains that had breached a polished surface showed Cr below the detection limit (<2 ppm Cr). The analysis showed the almost exclusive presence of Fe, with minor Mg and Mn and trace amounts of other elements. This indicates that the opaque black inclusions in these demantoids are actually magnetite. This assignment was further confirmed by Raman analysis on another grain and the attraction of several of the garnets to a handheld magnet. LA-ICP-MS analysis of the host demantoid also revealed very low Cr concentrations from below the detection limit to approximately 10 ppm. This was in stark contrast to the typically Cr-rich serpentinite-hosted demantoid from other deposits. Along with the presence of magnetite instead of chromite, this probably indicated the absence of significant Cr in the ultramafic protolith. While the internal features were very similar to those in other serpentinite-hosted demantoid, the presence of magnetite instead of commonly reported chromite was a surprising feature of this newly described material.

Aaron C. Palke and Vincent Pardieu  
GIA, Carlsbad and Bangkok

Figure 3. These magnetite and fibrous chrysotile inclusions are typical of the demantoids from this study. Field of view is 2.0 mm. Photomicrograph by Nathan Renfro.

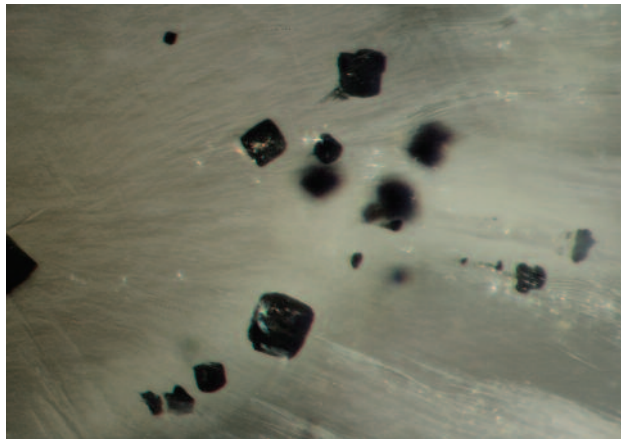


Figure 4. The Stayish black opal mine, active since 2013, is located in the Wollo province of northern Ethiopia.

**New deposit of black opal from Ethiopia.** Opal was first discovered in Ethiopia in the early 1990s. Specimens from Mezezo in the historical Shewa province consist of nodules of a reddish brown volcanic rock with orange, reddish brown, or “chocolate” brown precious opal inside. The next major discovery occurred in 2008, when white precious opal was found in the province of Wollo near Wegel Tena, about 550 km north of Addis Ababa (F. Mazzero et al., “Nouveau gisement d’opales d’Ethiopie dans la Province du Welo: Premières informations,” *Revue de Gemmologie a.f.g.*, No. 167, pp. 4–5). This deposit still produces large amounts of white and crystal precious opal and occasionally some black material (Winter 2011 Lab Notes, pp. 312–313).

In 2013, yet another source was discovered in Wollo, at the Stayish mine near the town of Gashena (figure 4). This discovery has yielded mostly dark and black opal, along with some white and crystal opal. Although it is only now being reported, the deposit has been actively producing since 2013. It is set in a distinct opal-bearing layer in a



Figure 5. While acidic ash layers occur repeatedly within the stratigraphic sequence at Stayish, precious black opal occurs only in this stratum. Photo by Pierre Hardy.

mountainous area at an altitude of around 3,000 meters. It lies approximately 700 km northeast of Addis Ababa, more than 100 km from the historic town of Lalibela by road, and about 30 km north of the white opal deposit.

Like the white opal, the black opal is found at the contact zone between the volcanic rock series and the underlying clay-rich layer (figure 5). The layer is one in a sequence of repeating volcanic ash and ignimbrite layers. Field observations at different locations show that the opal-bearing layer is contained in a single stratum extending for tens and even hundreds of kilometers along the mountain belt. The opal-bearing clay layer is about 60 cm thick and contains opal of various quality and color. The black opal is retrieved from flat tunnels up to 15–20 meters long that are dug horizontally into the mountain slope by local villagers. The material generally comes in nodules and chunks 2–5 cm long, but 10 cm pieces have also been retrieved from this deposit (figure 6).

The specimens are usually very dark, reminiscent of dyed or smoke-treated opal except that the surface does not show any staining in surface pits or fissures (figure 7). The stones also display a dark, even color all the way through and are sometimes layered with dark gray common opal. This separates it from sugar-acid treated opal (Winter 2011 GNI, pp. 333–334), where the darker color is confined to a more or less thick surface layer.

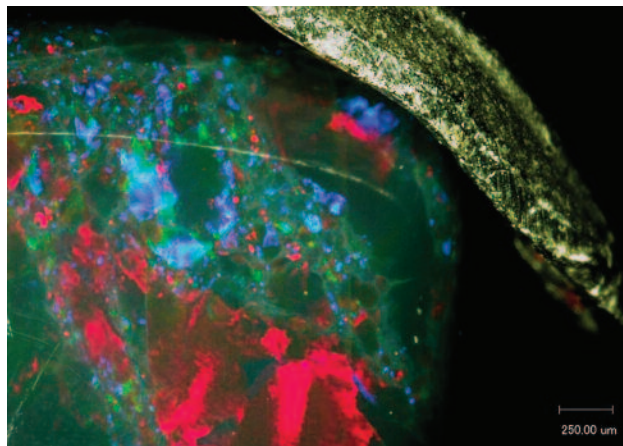
Initial X-ray fluorescence analyses showed barium (Ba) values ranging from below detection limit for one deposit with more crystal-like opal to 1000 ppmw for another de-



Figure 6. Pieces of black opal from the Stayish mine are usually 2–5 cm in diameter (bottom), though some may reach 10 cm in length (top). Photo by Tewodros Sintayehu.

posit with more dense and grayish material. The two deposits are on adjacent sides of the same mountain. The wide

Figure 7. This microscopic image of an Ethiopian black opal with surface scratches shows none of the black staining seen in smoke-treated or dyed opal. Some grayish non-precious opal material can be observed between the color patches. Photo by Hpone-Phyo Kan-Nyunt.



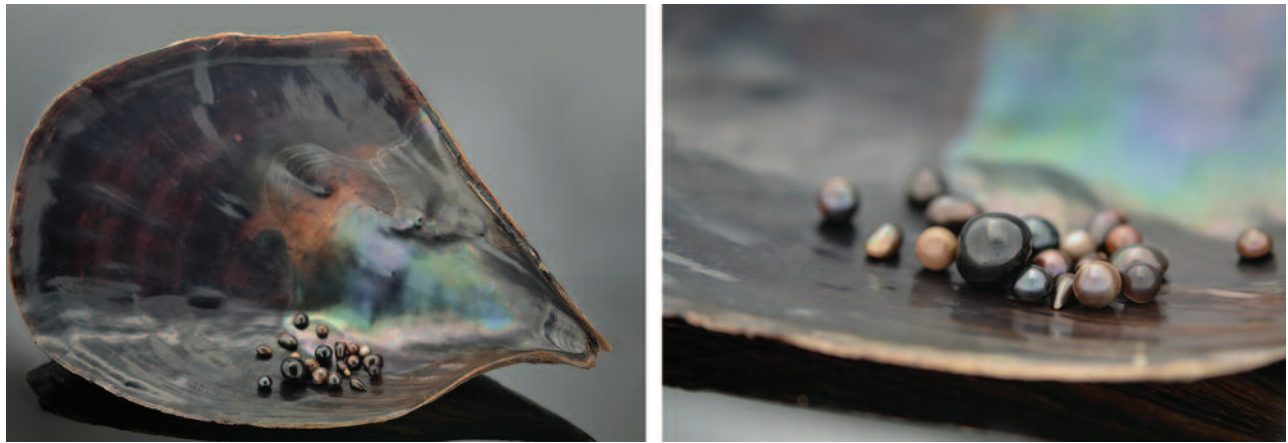


Figure 8. A parcel of natural pen pearls surrounds a 6.92 ct non-nacreous beaded cultured pearl. Photo by Olivier Segura.

range of Ba values confirmed the volcano-sedimentary character of the black opals, as previously described for white opals from Wegel Tena (B. Rondeau et al., “Play-of-color opal from Wegel Tena, Wollo Province, Ethiopia,” Summer 2010 *G&G*, pp. 90–105).

Preliminary studies with Fourier-transform infrared (FTIR) spectrometry did not give conclusive results due to the relatively opaque character of our samples. Raman spectra showed very strong carbon peaks, though these alone do not allow a reliable distinction between treated opal from Wegel Tena and natural-color black opal from the Stayish mine. Careful microscopic observation should reveal the natural character of opal from this new deposit, and further studies are in progress.

*Acknowledgments: The authors thank Mr. Bill Marcue from D.W. Enterprises for helping to finance this trip, as well as the Ministry of Mines of Ethiopia and the people of Wollo for their kindness and support.*

*Lore Kiefert and Pierre Hardy  
Gübelin Gem Lab, Lucerne, Switzerland  
Tewodros Sintayehu and Begosew Abate  
Orbit Ethiopia PLC, Addis Ababa, Ethiopia  
Girma Woldetinsae  
Ministry of Mines, Addis Ababa, Ethiopia*

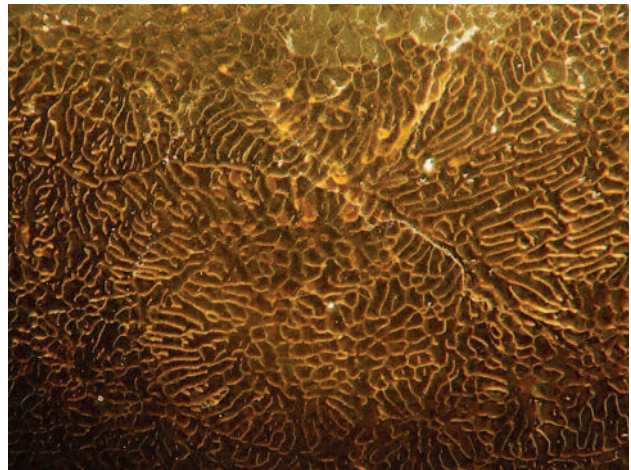
**The first identified non-nacreous beaded cultured pearl.** The Laboratoire Français de Gemmologie (LFG) recently had the opportunity to examine a collection of non-nacreous pearls from the Pinnidae family (*Pinna* and *Atrina* species). Among these, one black pen pearl drew our attention for its relatively large size: a 10.6–10.6 × 9.6 mm round button weighing 6.92 ct.

Its dark black porcelaneous appearance was typical of pearls from the calcitic part of *Atrina vexillum*, the kind usually submitted for laboratory analysis (figure 8). Observation at 85× magnification (figure 9) revealed a distinctive pattern of convolution, with a few micro-cracks.

Our findings on these cultured pearls are similar to those of N. Sturman et al. (“Observations on pearls reportedly from the Pinnidae family [pen pearls],” Fall 2014 *G&G*, pp. 202–215) in terms of Raman spectra (confirming the calcitic nature), UV-Vis spectra, and chemical composition.

The most interesting findings came from X-radiography. Microradiography/tomography imaging clearly shows a bright white disk inside the pearl (figure 10). The continuous separation line around this feature leaves no doubt that there is a bead inside the cultured pearl. As the beads used to nucleate “nacreous” pearls typically come from large freshwater mussels, we know that they are of a slightly denser material than saltwater nacre. Thus, they appear whiter than the surrounding material (of saltwater origin). The bead’s appearance was consis-

Figure 9. Surface magnification of the non-nacreous beaded cultured pearl revealed a typical calcitic pattern of pen pearls. Photo by Olivier Segura; magnified 85×.



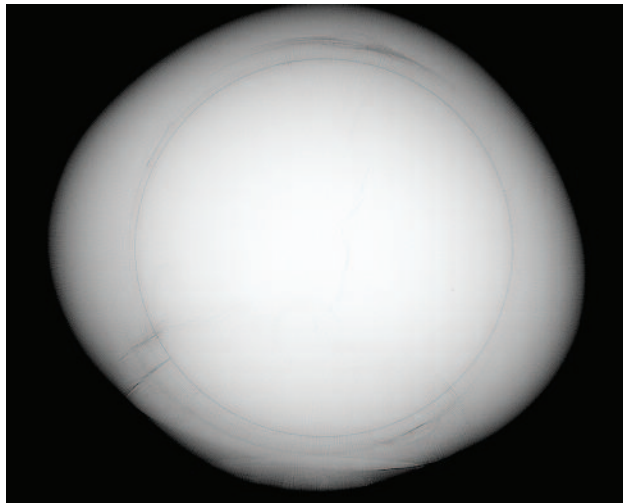


Figure 10. This microradiograph clearly identifies the pen pearl as a beaded cultured pearl. Image by Olivier Segura.

tent with a classical nucleus of the kind used in bead-nucleated pearls. Measurement of the bead gave a 6.70 mm diameter.

Tomography confirmed the presence of a near-perfect spherical bead inside the cultured pearl. Even with the owner's consent, however, we decided not to cut the pearl, as the imaging techniques were sufficient to prove the bead-cultured origin.

We wonder if this gem represents a single specimen achieved by a curious experimenter, or if there is now an industrialized process for cultivating such pearls. The cultivation technique used, even if it is known to produce cultured pearls in farms, requires advanced knowledge of the process. The owner reports having handled a black round pen pearl "the size of a golf ball." From the size and symmetry and given this new discovery of a bead-cultured pen pearl, one can speculate that this too might be a bead cultured pearl.

This bead nucleation technique for unusual species could have easily been developed in the past. To our knowledge, though, this specimen represents the first non-nacreous beaded cultured pearl examined by a laboratory. Faced with the expansion of the bead culturing process and the possibility of successful trials in different mollusks, gemologists need to be very cautious in natural origin determinations, even when there is every reason to believe a pearl to be natural.

Olivier Segura ([o.segura@bjop.fr](mailto:o.segura@bjop.fr))  
 Laboratoire Français de Gemmologie  
 Emmanuel Fritsch

## SYNTHETICS AND SIMULANTS

**An unusual doublet set in fine jewelry.** The Laboratoire Français de Gemmologie (LFG) examined a finely made



Figure 11. This green oval resembling an emerald proved to be a doublet with a beryl top and a topaz bottom. Photo by Olivier Segura.

white gold ring set with a green oval faceted stone that measured approximately  $20.2 \times 14.7 \times 8.6$  mm and resembled an emerald (figure 11). The stone showed distinct parallel growth zones, visible to the eye, under the table and the crown. These slightly undulating features (figure 12) were strongly reminiscent of Russian hydrothermal synthetic emerald (see, e.g., K. Schmetzer, "Growth method and growth-related properties of a new type of Russian hydrothermal synthetic emerald," Spring 1996 *G&G*, pp. 40–43).

The pavilion showed fingerprint-like inclusions consisting of droplets that were easily visible with the loupe (figure 13). This feature might lead one to believe it was a

Figure 12. Slightly undulating growth zones under the table and crown were reminiscent of Russian hydrothermal synthetic emerald. Photomicrograph by Alexandre Droux; magnified 80 $\times$ .





Figure 13. Fingerprint-like patterns reminiscent of flux synthetics are in fact very small two-phase liquid-gas inclusions. Photomicrograph by Alexandre Droux; magnified 80x.

flux synthetic emerald, inconsistent with the observations on the crown. Magnification reveals, however, that the fingerprint-like inclusions are actually made up of very small cavities, with bubbles that are clearly visible in the larger cavities. Therefore, the pavilion is actually a natural gem.

At the level of the girdle, close examination revealed one area with a separation line, hidden elsewhere because of the closed setting (figure 14). Through the table, small but prominent black spots occurred on a single plane. These were flat bubbles in cement introduced at the separation plane.

Only the crown appeared a weak red under the Chelsea filter. Under short-wave ultraviolet radiation, the upper part was inert while the lower part showed a light blue, milky luminescence. Under long-wave UV, both were inert. Therefore, the green oval was clearly a doublet (R. Webster, *Gems: Their Sources, Descriptions and Identification*, 4th ed., rev. by B.W. Anderson, Butterworths, London, pp. 457–468). The refractive index was impossible to measure on either the table or the pavilion because the prongs extended into these two areas.

Raman spectroscopy with a 514 nm laser and 4 cm<sup>-1</sup> resolution identified the crown as beryl and the pavilion as topaz. Hence the central stone of the ring is a doublet with a hydrothermal synthetic emerald top and a topaz bottom, which is quite unusual.

This case is consistent with an earlier report (J. Hyršl and U. Henn, "Synthetische smaragd-topas-dublette," *Zeitschrift der Deutschen Gemmologischen Gesellschaft*, Vol. 60, No. 3–4, pp. 111–112), which noted that the doublets were of Indian origin. The luminescence of the topaz bottom is slightly different in the present doublet, though still within the known variations of topaz luminescence.

Today far fewer doublets are being submitted to gemological laboratories. This specimen's unusual setting,

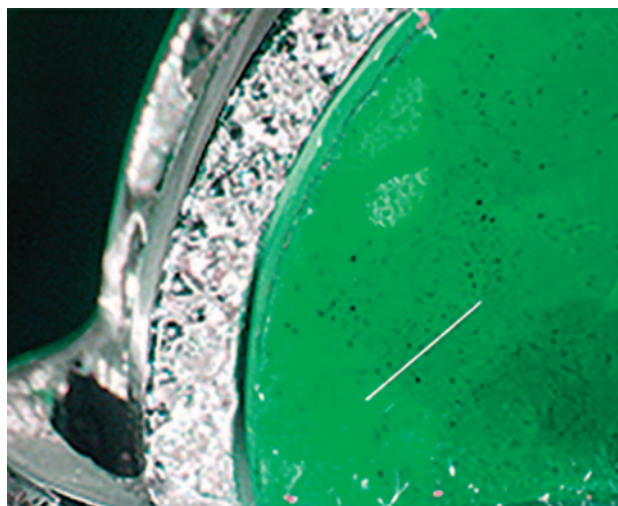


Figure 14. These small black spots are flat bubbles in cement along a separation plane. The line of separation was noticeable through the crown in only one area. Photomicrograph by Alexandre Droux; magnified 30x.

closed at the girdle and with large prongs preventing access to the table and pavilion for refractometer measurement, suggests an intent to disguise the composite (and partially synthetic) nature of the central gem. Even fine jewelry can be set with gems that are not natural, and gemologists should remain wary of doublets.

Alexandre Droux and Sophie Leblan  
 Laboratoire Français de Gemmologie (LFG), Paris  
 Emmanuel Fritsch  
 Jaroslav Hyršl  
 Prague

**Coated lawsonite pseudomorphs presented as chromian lawsonite.** Green (chromium-bearing) lawsonite first appeared on the mineral market in 2011–2012. It came from an undisclosed locality on the Greek island of Syros. The only large chromian lawsonite crystals previously documented are from Turkey (S.C. Sherlock and A.I. Okay, "Oscillatory zoned chrome lawsonite in the Tavsanli Zone, northwest Turkey," *Mineralogical Magazine*, Vol. 63, No. 5, 1999, pp. 687–692) and the western Alps (C. Mevel and J.R. Kienast, "Chromian jadeite, phengite, pumpellyite, and lawsonite in a high-pressure metamorphosed gabbro from the French Alps," *Mineralogical Magazine*, Vol. 43, No. 332, 1980, pp. 979–984). The maximum crystal size observed by Sherlock and Okay was approximately 500 microns, while Mevel's and Kienast's largest grains were only 200 microns in length. Interestingly, these grains were reported to be pink. Samples available online ranged from US\$50 to more than US\$350, and all were reported to be from Syros. To the best of our knowledge, chromian lawsonite is not available from other localities.

We purchased a chromian lawsonite sample purport-



Figure 15. These large green crystals were reported as chromian lawsonite. Ankerite (orange) and actinolite (light green) are the major matrix minerals between the large green crystals (verified by Raman spectroscopy). The specimen is 4.8 cm long. Photo by Earl O'Bannon.

edly from Syros for mineralogical analysis (figure 15). The sample measured  $4.8 \times 2.8 \times 2$  cm, and its largest crystal was about 1.5 cm in length. The crystals were deep green and present in a matrix dominated by ankerite and actinolite. Our sample appeared similar to most other chromian lawsonite samples available for purchase online.

Initial microscopic observations of the large green crystals revealed a smooth wavy surface (figure 16). Raman analysis of this surface showed peaks at 1301, 1342, 1451, and 2720  $\text{cm}^{-1}$  and a broad peak at 2800–3000  $\text{cm}^{-1}$  with secondary peaks at 2871, 2932, and 2961  $\text{cm}^{-1}$  (figure 17). These peaks are typical of Group B fillers (strong aliphatic peaks), which have been used to enhance the appearance of emeralds (M.L. Johnson et al., "On the identification of various emerald filling substances," Summer 1999 *G&G*, pp. 82–107). The absence of Raman peaks in the approximately 1600  $\text{cm}^{-1}$  region indicates that this coating is not likely a Group A, C, D, or E filler (Johnson et al., 1999; L. Kiefert et al., "Raman spectroscopic applications to gem-

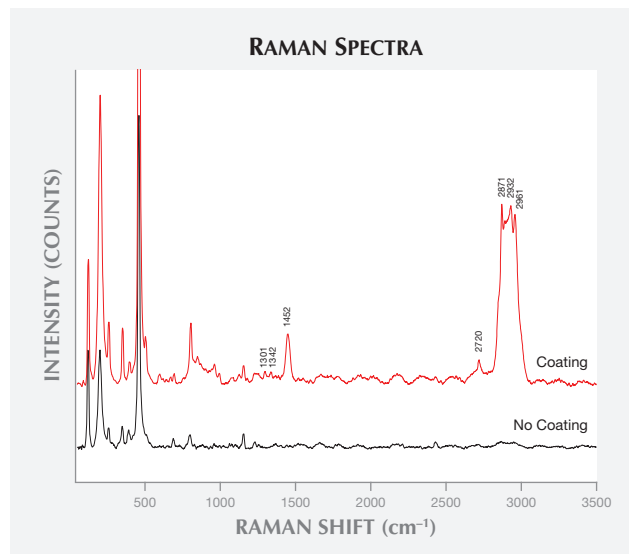
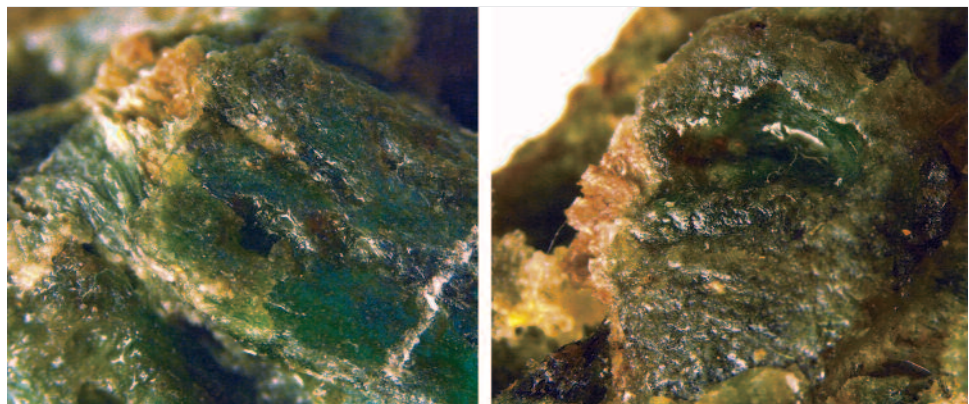


Figure 17. Raman spectra of the coating before and after cleaning the surface with acetone. Spectra were taken in the same location, with an approximately 2 micron spot size. The typical Raman spectrum of quartz, with clinocllore contamination, is observed in the low-frequency region. Spectra are offset for clarity.

mology," *Handbook of Raman Spectroscopy*, Vol. 28, 2001, pp. 469–490). This smooth surface was waxy to the touch and easily scratched with a fingernail, and wiping it off with acetone revealed a light green to white surface. All peaks associated with this coating disappeared after cleaning with acetone (again, see figure 17).

After the coating was removed, Raman analysis of the formerly dark green crystals revealed spectra corresponding to the minerals muscovite/phengite, clinocllore, and quartz (figure 18). About a hundred measurements were taken of all the large green crystals in the sample at the 2 micron scale-length, and no evidence of lawsonite was found. This assemblage of minerals is common in lawsonite pseudomorphs from Syros; prograde pseudomorphs, also containing zoisite and 0.5–3.0 cm in size, are reported

Figure 16. The photo on the left (magnified 1.25 $\times$ ) shows a fingernail scratch on the surface. The photo on the right (magnified 1.6 $\times$ ) shows pooling of the coating in a depression in the grain. Photos by Earl O'Bannon.



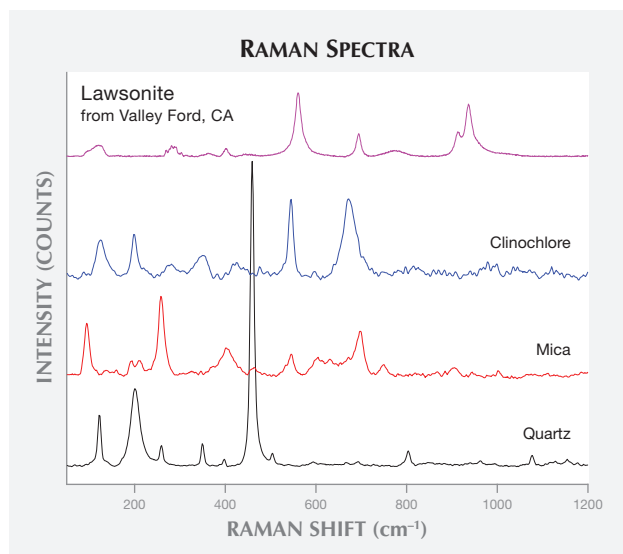


Figure 18. Raman spectra of acetone-cleaned large green crystals (bottom three spectra). Mica and clinocllore are the most abundant minerals in the large green crystals. The reference lawsonite spectrum is for a sample from the UCSC mineral collection (sample no. 6481), from Valley Ford in Sonoma County, California. Spectra offset for clarity.

to be abundant in this locale (J.B. Brady et al., "Prograde lawsonite pseudomorphs in blueschists from Syros, Greece," *GSA Annual Meeting*, 2001, paper 105-0).

We conclude that this sample is composed of lawsonite pseudomorphs, which were coated to make them appear deep green and imitate chromian lawsonite crystals. The euhedral crystals consisted of a fine-grained mixture of muscovite, clinocllore, and quartz. It is not known whether this sample was coated with the recognition that these were lawsonite pseudomorphs.

All samples of chromian lawsonite that we have found for purchase are from Syros. Thus, buyers should be aware that these could potentially be artificially coated lawsonite pseudomorphs. Further analysis of other "chromian lawsonite" samples is required to document whether any true chromian lawsonites from this locality actually exist.

*Acknowledgments:* Drs. Hilde Schwartz and Elise Knittle provided helpful discussions about pseudomorphs, and Chelsea Gustafson (UCSC Chemistry Department, Partch Lab) assisted with the microscope used to take images of the coating. The UCSC Mineral Physics Lab is supported by the NSF.

Earl O'Bannon and Quentin Williams  
University of California, Santa Cruz

**Unusual composite ruby rough.** The Indian Gemological Institute – Gem Testing Laboratory recently examined an unusual 14.77 ct specimen that resembled ruby rough. Initial gemological testing (RI, hydrostatic SG, optical properties, visible spectrum, and infrared spectroscopic analysis)

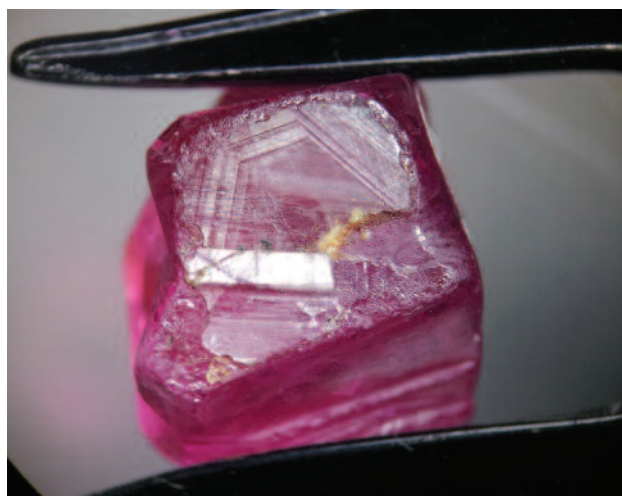
was consistent with ruby.

The rough was partially polished on two opposite sides, where hexagonal growth zoning was easily visible with the unaided eye (figure 19). Several striations and grooves were visible on the side of the rough.

The pattern and nature of these grooves raised suspicion about the rough's origin. Closer examination under magnification revealed that hexagonal zoning and fine silk on the partially polished surfaces were confined to a depth of approximately 1.5 mm. Two thin slabs of about 1.5 mm each appeared to be attached to the two opposite ends of the rough. No other inclusions were found under magnification. We did observe a slight difference in the color of the thin layer and the main body. The thin slabs were purplish red, while the main body was pinkish red. Since the hexagonal zoning was within the thin slabs and the physical properties were consistent with ruby, we concluded that they were natural ruby slabs. The natural ruby slabs were pasted with a glue that made them appear orangy in transmitted light, and trapped gas bubbles were also observed in the junction plane (figure 20). The two natural slabs were polished to show the hexagonal zoning, while the rest of the rough was kept coarse to restrict views of the interior. Fine triangular grooves were engraved on the rough's surface to imitate the natural growth markings of ruby.

Under magnification, a small cluster of gas bubbles was visible through one of the smooth grooves on the specimen's main body, evidence of synthetic origin. Several fractures were also present in the rough, probably an attempt to imitate fingerprint inclusions. Under short-wave UV, the natural slabs fluoresced red while the synthetic ruby

Figure 19. The 14.77 ct composite ruby rough was partially polished on opposite sides where natural ruby slabs were pasted to a synthetic ruby crystal. Notice the hexagonal zoning on the polished surface. Photo by Meenakshi Chauhan; magnified 15 $\times$ .



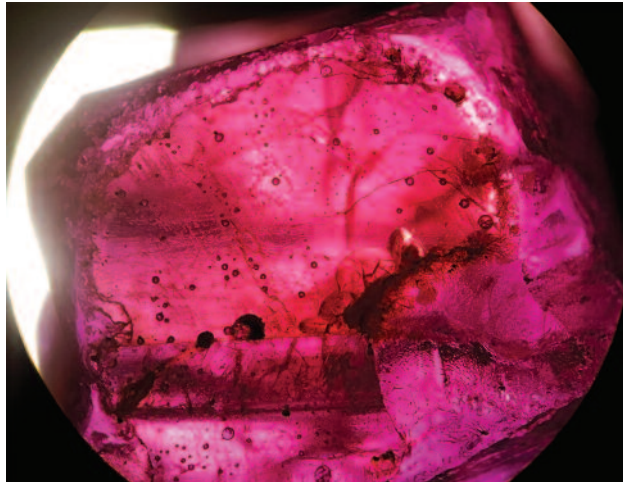


Figure 20. In transmitted light, the natural ruby slab appeared orangy due to the adhesive. Trapped gas bubbles are seen in the junction plane. Photo by Meenakshi Chauhan; magnified 30x.



Figure 21. Under short-wave UV light, the synthetic ruby portion of composite rough fluoresced chalky while the natural ruby slabs fluoresced red. Photo by Meenakshi Chauhan.

rough showed a strong chalky fluorescence (figure 21). Chalky fluorescence was further evidence of the rough's synthetic origin.

Cut and polished composites are regularly encountered, but a composite where synthetic rough is fashioned to imitate natural gem material poses a more significant challenge.

Meenakshi Chauhan ([meenakshi@gjepcindia.com](mailto:meenakshi@gjepcindia.com))  
 Indian Gemological Institute –  
 Gem Testing Laboratory, Delhi

**Dyed green marble imitating jadeite.** A client of the Lai-Tai An Gem Lab in Taipei recently submitted for identification what was claimed to be a piece of fine jadeite mounted in a yellow metal pendant (figure 22). The oval cabochon measured 39.8 × 29.8 mm and exhibited a homogenous green color. At first glance, it bore a strong resemblance to jadeite. While dyes, polymer treatments, or a combination of the two are commonly applied to jadeite—and dyed green quartzite is sometimes used to imitate green jadeite and other materials such as glass and plastic—this piece proved to be dyed green marble with calcite as the main mineral. This was the first time dyed marble had been represented to us as jadeite.

Although marble is fairly abundant, calcite's low hardness and easily visible cleavages do not make it a viable substitute for jadeite. Yet it does lend itself well to carving. Chinese merchants often sell untreated carved marble by the trade names "Hanbai jade" or "Afghanistan jade," or even offer such material as "antique jade." Jade, pronounced "yu" in Chinese, is a general term that typically applies to aggregates of minerals. Marble in the Chinese jewelry market is frequently fashioned into bangles and carved pendants, and some may subsequently be dyed or

partially dyed to imitate jadeite jade. Although it was impossible to calculate the SG of this mounted specimen, calcite's RI of 1.65 overlaps with jadeite jade's, leading to the possible misidentification of such material (J.M. Hobbs, "The jade enigma," Spring 1982 *G&G*, pp. 3–19).

The identification was determined using Raman and FTIR spectroscopy. The sample showed Raman peaks at around 1084, 712, 275, and 145  $\text{cm}^{-1}$  (figure 23), with IR

Figure 22. This was claimed to be a high-quality piece of jadeite jade mounted in a yellow metal pendant. The oval cabochon measured 39.8 × 29.8 mm, exhibited a homogenous green color, and on first impression appeared to resemble jadeite. Photo by Lai Tai-An Gem Lab.



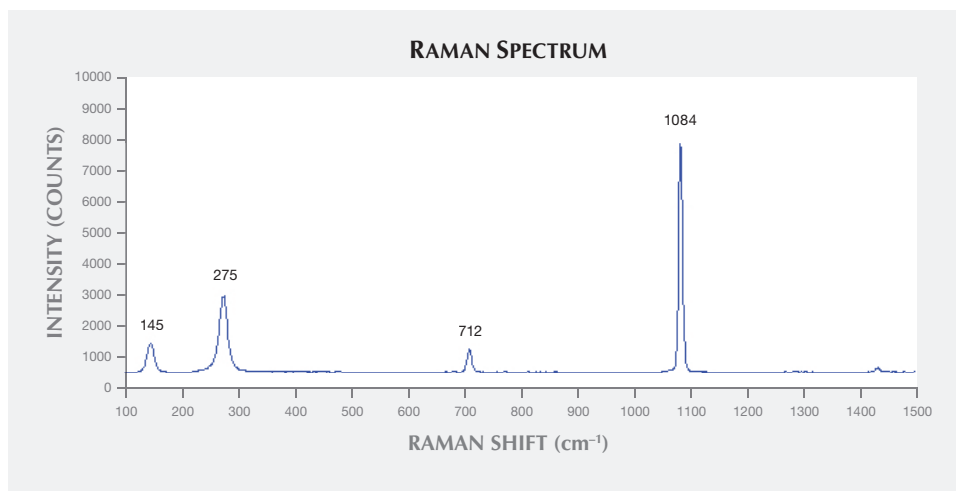


Figure 23. Raman peaks at around 1084, 712, 275, and 145  $\text{cm}^{-1}$  were consistent with calcite.

peaks at around 1445 and 878  $\text{cm}^{-1}$ . Microscopic observation revealed a network of dyed grain boundaries (figure 24). The dye treatment was confirmed with the spectroscope, where a single broad band typical of some green dyes was clearly evident in the red-orange region. Long-wave UV did not offer any distinction. Although destructive tests are always avoided, the client allowed us to gently scratch the surface with a metal pointer, which confirmed the material's low hardness. This submission reinforces the need to consider all types of material when dealing with items resembling jadeite.

Larry Tai-An Lai ([service@laitaian.com.tw](mailto:service@laitaian.com.tw))  
Lai Tai-An Gem Laboratory, Taipei

**Dyed marble as a purple sugilite imitation.** In the past two years, many sugilite products with a dark purple color and an obvious granular texture have appeared in the Chinese

Figure 24. Microscopic observation revealed a network of dyed grain boundaries. Photo by Lai Tai-An Gem Lab; magnified 50 $\times$ .



market. Sugilite pendants and bangles are very popular. Their internal texture and color distribution are inconsistent with previously documented natural specimens and suggest dyed artifacts. With that in mind, we obtained a "sugilite" bangle to investigate its gemological characteristics.

The bangle weighed about 71 grams and had a dark purple color that was distributed along the mineral grain boundaries (figure 25). Spot RIs of 1.48, 1.53, 1.57, and 1.63 were obtained from different areas of the bangle. Its hydrostatic SG was about 2.65, significantly lower than that of natural sugilite. The sample fluoresced strong purple and medium red under long- and short-wave UV radiation, respectively, which indicated treatment with organic dye(s). Five main peaks were observed in the 1600–700  $\text{cm}^{-1}$  region of the FTIR spectrum (figure 26). The three peaks at 1427, 881, and 710  $\text{cm}^{-1}$  are typical for calcite. The remaining two peaks at 1530 and 1505  $\text{cm}^{-1}$  were believed to result from an organic dye.

Figure 25. Testing of this bangle identified it as a dyed marble imitation of purple sugilite. Photo by Shan-shan Du.



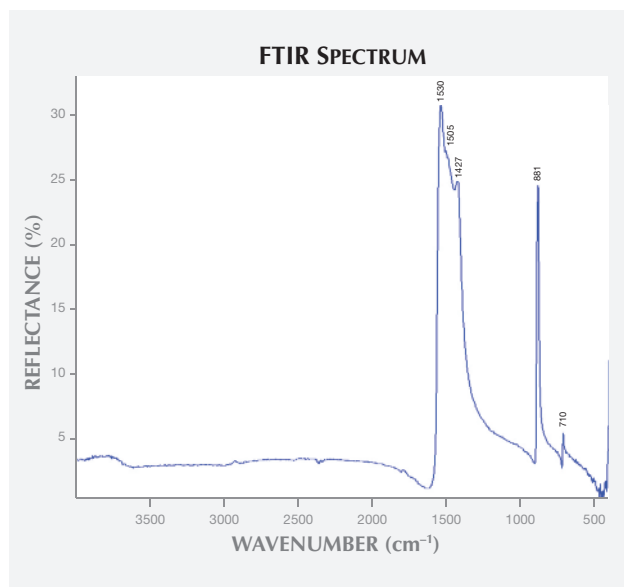


Figure 26. The FTIR spectrum of the purple bangle contained characteristic peaks at 1427, 881, and 710  $\text{cm}^{-1}$  that are typical for calcite.

Although the imitation resembles sugilite, its internal texture, RI, SG, fluorescence, and FTIR spectrum identify it as marble. Since marble usually occurs as a mineral aggregate with a loose texture, it is easily dyed to imitate other precious gemstones. We can therefore expect to see a steady influx of marble imitations in the market, and rigorous testing will be needed to protect consumers.

Ke Yin and Shan-shan Du  
China University of Geosciences, Wuhan, China

#### Unusual short-wave UV reaction in synthetic blue spinel.

The Indian Gemmological Institute – Gem Testing Laboratory recently examined a 1.44 ct blue oval mixed cut specimen (figure 27). Standard gemological testing revealed the following properties: RI—1.728; hydrostatic SG—3.64; strong anomalous double refraction under the polariscope; Chelsea filter reaction—strong red; and red transmission in fiber-optic light. The sample showed general absorption bands between 535–550, 560–590, and 615–635 nm in the handheld spectroscope. Microscopic examination with a fiber-optic light source revealed shiny dotted inclusions that were scattered and created a wavy pattern; in some areas, the dotted inclusions were arranged in a series (figure 28). This wavy pattern has not been reported in natural spinel. The author has seen this pattern in some Verneuil synthetic spinel. There is a possibility that these inclusions might be very minute gas bubbles or unmelted feed powder.

These properties—higher RI, higher SG, red Chelsea filter reaction, anomalous double refraction, and absorption spectrum features—are diagnostic features of cobalt-doped synthetic blue spinel grown by the Verneuil (flame-fusion) process (M. O’ Donoghue, *Synthetic, Imitation & Treated*



Figure 27. This 1.44 ct synthetic spinel was grown by the Verneuil process but displayed the short-wave UV reaction of a flux-grown sample. Photo by Pragati Verma.

*Gemstones*, Butterworth-Heinemann, Oxford, UK, 1997, p. 153).

When tested with UV, this synthetic spinel had an unusual reaction. Under both long- and short-wave UV, the

Figure 28. Series of dotted inclusions were seen in some areas of the synthetic spinel. The dots were so concentrated that it was difficult to distinguish them individually. Photomicrograph by Pragati Verma; magnified 25 $\times$ .





Figure 29. The synthetic spinel displayed red fluorescence under short-wave UV. Photo by Pragati Verma.

sample showed red fluorescence (figure 29). This was an unexpected short-wave UV reaction for Verneuil-grown blue synthetic spinel, which generally shows a mottled blue to bluish white reaction. This kind of fluorescence was observed in synthetic blue spinel grown by a flux method (S. Muhlmeister et al., "Flux-grown synthetic red and blue spinels from Russia," Summer 1993 *G&G*, pp. 81–98).

Pragati Verma  
Indian Gemological Institute –  
Gem Testing Laboratory, Delhi

## MARKET REPORT

**Online diamond sales 17% of U.S. market.** A recent De Beers study reported that worldwide retail sales of diamond jewelry totaled \$79 billion in 2013, up \$5 billion on a 7% increase in U.S. demand and a 12% increase in China.

Online sales of diamond jewelry comprise about 17% of the market in the U.S., according to the study. These sales include both strictly online companies such as Blue Nile and traditional retailers who also sell over the Internet.

The De Beers report also noted that 25% of Chinese consumers now research prospective diamond purchases online before making an actual purchase and that the number of retail stores selling diamond jewelry increased 30% from 2010 to 2013. There are, however, strong signs that the heady growth is beginning to slow, according to De Beers. Retailers in Guangdong Province reported that sales declined 5.1% for the first eight months of 2014, while sales of gold pieces nationwide fell 9.1% during that period, according to a government report.

In the U.S., the Department of Commerce reported that jewelry and watch sales from all sales channels increased 4.9% in August, compared to the same month in 2013. This rise reflects even greater sales volume because prices for gold and diamonds declined several percentage points in 2014.

De Beers noted that diamond production increased 7% to 145 million carats, still well under the 2005 peak of 175

million carats. It also predicted that production would decline, despite new sources coming on stream, because older mine deposits are becoming more costly to work as operations go deeper and ore grade declines.

Russell Shor  
GIA, Carlsbad, California

**Record prices at gem auctions.** Auction records kept breaking in late 2014 as the world's ultra-wealthy buyers vied for rare, important gemstones. At Sotheby's October 7 Hong Kong auction, an 8.41 ct GIA-graded Fancy Vivid purple-pink, Internally Flawless diamond (figure 30) drew a winning bid of \$17,768,041 from a private buyer from Asia. It was the highest price ever paid for a Vivid pink diamond at auction. And at \$2.1 million per carat, it came close to besting the all-time per-carat price achieved by a gemstone.

On November 21 at Sotheby's New York, a 9.75 ct Fancy Vivid blue diamond (figure 31) sold for \$32,645,000, a new auction record total price for any blue diamond. At \$3,348,205 per carat, it was also a new record price per carat for any diamond. The pear-shaped diamond went to a private collector in Hong Kong who named it the Zoe diamond.

Russell Shor

## ANNOUNCEMENTS

**Pearl newsletter: *Margaritologia*.** The Greek word for pearl, *margaritēs*, was used by Theophrastus in the fourth century BC in the first known effort to explain the scientific origin

Figure 30. This 8.41 ct pear-shaped Fancy Vivid purple-pink diamond sold for more than \$17.7 million at Sotheby's Oct. 7 auction in Hong Kong. Photo courtesy of Sotheby's.





Figure 31. This 9.75 ct Fancy Vivid blue diamond sold at Sotheby's November 21 auction in New York for more than \$32.6 million, a record total price for blue diamonds and a record per-carat price for any diamond. Photo courtesy of Sotheby's.

of the beloved organic gem. *Margaritologia*, or "the science of pearls," is a newsletter recently launched by Elisabeth Strack, founder and director of Gemmologisches Institut Hamburg and author of the comprehensive book *Pearls*. Ms. Strack is also a member of *G&G's* editorial review board.

The newsletter, published four times a year in English and German, in print and electronic versions, offers a forum for pearl research findings and news. Topics range from science and history to pearl grading and testing, farming, and market conditions. The first issue, published in October, featured articles on Vietnamese cultured pearls, DNA fingerprinting of pearls, the International Gemmological Conference in Hanoi, *Spondylus* pearls, a Mikimoto necklace, and a museum exhibition in Mecklenburg, Germany.

A yearly subscription to *Margaritologia* is €70, with a discounted rate for CPAA or NAJA members. More information can be found at [www.gemmologisches-institut-hamburg.de](http://www.gemmologisches-institut-hamburg.de).

Erin Hogarth  
San Diego, California

## CONFERENCE REPORT

**Gem session at 2014 GSA meeting.** A full-day session on gem materials was held Oct. 20, 2014, in conjunction with the annual meeting of the Geological Society of America (GSA) in Vancouver.

The morning presentations focused mainly on diamonds. **Thomas Stachel** (University of Alberta) summarized work to constrain the geological conditions of diamond formation. It is thought to have formed in the mantle from an oxidized carbonate-bearing fluid with high carbon and low nitrogen concentrations. **Eloise Gaillou** (Natural History Museum of Los Angeles County) discussed pink diamonds whose color originates from narrow lamellae created by plastic deformation parallel to the octahedral growth planes. These lamellae contain a high density of luminescent defects along with localized strain. As a result of plastic deformation in the mantle, these diamonds accommodate stress along the lamellae by mechanical twinning. The unidentified optical defects responsible for the pink coloration are also created by this deformation. **Richard Wirth** (Geo-ForschungsZentrum) described the use of a transmission electron microscope with a focused ion beam to characterize microstructures in materials. Blue color in quartz is caused by Rayleigh scattering from submicron- and nanometer-sized inclusions of mica, ilmenite, and rutile. The black color of carbonado diamond results from its polycrystalline nature and partially open grain boundaries that cause internal total reflection of light. Cloud-like inclusions in Madagascar sapphires are due to nanocrystalline titanium-rich oxide inclusions. **Wuyi Wang** (GIA) discussed the use of carbon isotope analysis to help distinguish natural diamonds from CVD-grown synthetic diamonds. He found no overlap in isotope composition between them, but within the synthetic diamonds there was variation between manufacturers and even from the same manufacturer. **Karen Smit** (GIA) described interesting features of diamond crystals from Marange, Zimbabwe, which display both cuboid and octahedral growth sectors and distinctive center-cross patterns (often highlighted by graphite-particle clouds). **Mike Breeding** (GIA) reviewed the properties of certain treated-color diamonds. Electron irradiation yields green colors in diamonds with higher nitrogen content, and blue colors in diamonds with lower amounts of nitrogen. Characterization of their optical defects provides a means of distinguishing them from natural-color diamonds. **Troy Ardon** (GIA) characterized some optical defects in hydrogen-rich diamonds from Zimbabwe. Spectral features associated with certain defects could be correlated with noticeable clouds in these diamonds. **Robert Luth** (University of Alberta) discussed a model of diamond formation in the mantle. He suggested that it takes place as carbon-hydrogen-oxygen (CHO) fluids rise in the lithosphere during isobaric cooling, or combined cooling and decomposition. This model helps explain a number of observations regarding the geologic occurrence of diamonds. **Mandy Krebs** (University of Alberta) discussed

size frequency distribution as a predictive tool for macro-diamond grade at Canada's Ekati mine. She found that Ekati diamonds of different size fractions display broadly similar nitrogen and carbon-13 isotope compositions. **Mederic Palot** (University of Alberta) studied diamonds from the Kankan deposit in Guinea that are believed to have formed at great depths (>300 km in the mantle). Characterization of nitrogen and carbon isotopes indicates rapid ascent from the mantle to shallower depths. **Charles Kosman** (University of British Columbia) studied the chemical composition of mineral inclusions in alluvial diamonds from the Kasai area of Congo. These diamonds originated from the kimberlites around Lucapa in neighboring Angola, which contain a significant proportion (~ 20%) of eclogitic diamonds.

The afternoon session covered a range of topics. **Lee Groat** (University of British Columbia) reviewed Canadian gem minerals. In addition to diamond, the country is an important source of nephrite jade, ammolite, and amethyst. Recent discoveries of ruby, sapphire, spinel, and emerald also show promise. **David Newton** (University of British Columbia) analyzed peridotite and pyroxenite xenoliths from the Muskox kimberlite in northern Canada to better understand the rock types in the underlying mantle. **Howard Coopersmith** (Fort Collins, Colorado) described a placer deposit at Mount Carmel in Israel that has yielded diamond, ruby, sapphire, and natural moissanite crystals and fragments that appear to have originated from different igneous and metamorphic source rocks. **Aaron Palke** (GIA) presented a trace-element study of demantoid garnet as the basis for distinguishing this important gem material from different geologic and geographic sources. **Cigdem Lule** (Glenview, Illinois) discussed the need for a more systematic approach to gem nomenclature, which is often determined by jewelry trade practices, as opposed to the more rigorous procedure used for assigning new mineral names. **Nancy McMillan** (New Mexico State University) presented a multivariate chemical analysis of tourmaline, a mineral that can be an exceptional provenance indicator in detrital sediments. This analysis has proven successful in assigning tourmaline samples to different geologic environments. **David Turner** (University of British Columbia) conducted a study of sapphires and associated minerals from the marble-hosted Beluga occurrence in northern Canada by hyperspectral imaging over the 550–2500 nm range. This technique could be useful in the field for analyzing rock samples and in airborne surveys over terrain with good rock exposures. **Philippe Belley** (University of British Columbia) studied blue calcite skarn deposits in Ontario and Quebec. Their geologic setting and low iron content make them potential sources of grossular garnet and other gem minerals. **J.N. Das** (Geological Survey of India) reviewed the exploration and mining of diamonds and colored gemstones throughout India. **Andrew Fagan** (University of British Columbia) described the Aappaluttoq ruby and pink sapphire deposit in Greenland. Based on field studies, it appears to be the world's largest geologically defined gem corundum deposit, with an estimated 400 million carats of material within 65 meters of the surface. Commer-

cial mining is expected to begin in 2015. **Sytle Antao** (University of Calgary) studied optical anisotropy in cubic garnets, which has been recognized for more than a century but remains incompletely understood. X-ray diffraction study of several anisotropic samples revealed they contain two or three cubic phases with slightly different structural parameters. The intergrowth of these phases on a nano-domain scale produces the strain-induced optical anisotropy. **Barbara Dutrow** (Louisiana State University) discussed how tourmaline, an important accessory mineral in many geologic environments, can be used to help locate gem deposits.

In the separate poster session, **Ellen Svadlenak** (Oregon State University) and co-authors used electron microprobe analysis to study variations in the trace elements in emeralds from Muzo, Colombia. **Lauren Forbes** (Western Washington University) and co-authors analyzed emeralds from four different Muzo mines using SEM-CL (cathodoluminescence) along with LA-ICP-MS to better understand the chemical and physical conditions for their growth. All emeralds tested showed a strong red luminescence. The researchers concluded that Muzo emeralds are compositionally unique. **Gena Philibert-Ortega** (Murrieta, California) and co-authors described the scientific influence of James Sowerby's rare five-volume *British Mineralogy* in the early 19th century. **Elise Skalwold** (Cornell University) and co-authors reviewed their research on a highly unusual blue inclusion in a diamond. While it was identified as olivine, the reason for the blue color remains a mystery.

An overview of the gem research session from the 2014 GSA meeting is available at <https://gsa.confex.com/gsa/2014AM/webprogram/Session35272.html>.

*James E. Shigley and Dona M. Dirlam  
GIA, Carlsbad*

## ERRATA

1. The cover of the Fall 2014 issue listed the volume number as 49 rather than 50.
2. In the Fall 2014 lead article on the Sri Lankan gem and jewelry industry, the figure 4 caption (p. 176) should have acknowledged that the two sapphire crystals in the photo are courtesy of Bill Larson (Pala International, Fallbrook, California).
3. Also in the Fall 2014 issue, table 2 of the pen pearls article (p. 211) listed an incorrect value. For pearl sample 3, the <sup>88</sup>Sr composition was 806 ppmw, not 8067 ppmw.
4. In the Summer 2014 article on three-phase inclusions in emerald, the log-log plots in figures 24 and 25 (pp. 129 and 131) contained labeling errors on the x-axis scales. For figure 24, the Fe concentration scale should have extended from 100 to 10,000 ppmw rather than 10 to 1,000 ppmw. In figure 25, the Fe concentration scale should have extended from 100 to 100,000 ppmw rather than 100 to 1,000 ppmw.